

EFFECT OF THE GREEN-EMITTING $\text{CaF}_2:\text{Ce}^{3+},\text{Tb}^{3+}$ PHOSPHOR PARTICLES' SIZE ON COLOR RENDERING INDEX AND COLOR QUALITY SCALE OF THE IN-CUP PACKAGING MULTICHIP WHITE LEDs

N. H. K. NHAN^a, T. H. Q. MINH^{a*}, T. N. NGUYEN^b, M. VOZNAK^b,
V. V. HUYNH^c

^a*Optoelectronics Research Group, Faculty of Electrical and Electronics Engineering, Ton Duc Thang University, Ho Chi Minh City, Vietnam*

^b*VSB-Technical University of Ostrava, 17. listopadu 15/2172, 708 33 Ostrava - Poruba, Czech Republic*

^c*Faculty of Electrical and Electronics Engineering, Ton Duc Thang University, Ho Chi Minh City, Vietnam*

In this paper, we investigate the effect of the green-emitting $\text{CaF}_2:\text{Ce}^{3+},\text{Tb}^{3+}$ phosphor particle's size on the color rendering index (CRI) and the color quality scale (CQS) of the in-cup packaging multichip white LEDs (MCW-LEDs). For this purpose, 7000K and 8500K in-cup packaging MCW-LEDs is simulated by the commercial software Light Tools. Moreover, scattering process in the phosphor layers is investigated by using Mie Theory with Mat Lab software. Finally, the research results show that the green-emitting $\text{CaF}_2:\text{Ce}^{3+},\text{Tb}^{3+}$ phosphor's size crucially influences on the CRI and CQS. From that point of view, $\text{CaF}_2:\text{Ce}^{3+},\text{Tb}^{3+}$ can be proposed as a potential practical direction for manufacturing the in-cup packaging phosphor WLEDs.

(Received November 10, 2017; Accepted April 2, 2018)

Keywords: WLEDs; Green-emitting, $\text{CaF}_2:\text{Ce}^{3+},\text{Tb}^{3+}$ phosphor; CRI; CQS; Mie Theory

1. Introduction

In the last few years, the white light emitting diodes (LEDs) have many advantages in energy efficiency, long lifetime, compactness, environment-friendly and designable features in comparison with incandescent and fluorescent lamps. In the last few decades, the efficiency of white LEDs lighting had already exceeded that of the incandescent lamps and was competitive with fluorescent lamps. Without a doubt, the white LEDs lighting has been setting foot in the lighting industry and dramatically challenges the conventional lighting [1-3]. Industrial technology system of solid state lighting mainly includes four critical technological fields: epitaxy material technology, chip design and manufacturing (upstream industry), packaging materials (midstream industry) and process technology and system integration technology and applications (downstream industry). [1-5]. In the midstream LEDs industry, the white light consists of transmitted chip-emitted blue rays and phosphor-converted yellow rays in phosphor coating layer. Obviously, phosphor coating structure plays a vital role in affecting illumination quality of WLEDs. Packaging not only can ensure better performance of LED devices by enhancing reliability and optical characteristics but can also realize control and adjustment of the final optical performance [6-8]. There are many studies concentrate on improving the color uniformity, and the luminous efficacy of WLEDs by controlling the packaging process. Moreover, the lighting properties of LEDs were significantly improved by using phosphors $\text{Sr}_{1-x}\text{Ba}_x\text{Si}_2\text{O}_7:\text{Eu}^{2+}$ (0<x<1) [9] and by using $\beta\text{-SiAlON}:\text{Yb}^{2+}$ phosphor [11], or by varying phosphor materials and packaging structures [10], or by Red-Emitting Phosphor $\text{Li}_2\text{SrSiO}_4:\text{Eu}^{3+},\text{Sm}^{3+}$ [11], by adding the red or green phosphor to YAG:Ce phosphor compound of W-LEDs [12-15]. Then the LEDs packaging and its materials research are the critical directions in LEDs manufacturing.

* Corresponding author: tranhoangquangminh@tdt.edu.vn

In this research, we investigate the influence of the green-emitting $\text{CaF}_2:\text{Ce}^{3+}:\text{Tb}^{3+}$ phosphor particle's size on the color rendering index (CRI) and the color quality scale (CQS) of the in-cup packaging MCW-LEDs.

The main contributions of this paper can be summarized as the followings:

1) The green-emitting $\text{CaF}_2:\text{Ce}^{3+}:\text{Tb}^{3+}$ phosphor particle's size significantly affects the color uniformity of the MCW-LEDs.

2) The CRI and CQS of MCW-LEDs can be increased from 58 to 66 and 55 to 65, respectively.

The rest of this research can present as below. The second section simulates the physical model MCW-LEDs and proposes the mathematical description of the proposed model. The simulation results are presented, and some discussions are proposed in the third sections. Finally, section IV concludes this paper.

2. Research Model MCW-LEDs and Mathematical Description

2.1. Physical Model WLEDs

In this section, we simulate the real 7000K, and 8500K MCW-LEDs by the commercial software Light Tools based on the Monte Carlo ray-tracing method (Fig. 1). In this physical model of MCW-LEDs, the reflector has a bottom length of 8 mm, a height of 2.07 mm and a length of 9.85 mm at its top surface. The remote phosphor layer with a fixed thickness of 0.08 mm covers the 9 LED chips. Each LED chip with a square base of 1.14 mm and a height of 0.15 mm is bound in the cavity of the reflector shown in Fig. 1. The radiant flux of each blue chip is 1.16 W at wavelength 455 nm [12-14]. In this section, the size of the green phosphor particle was changed from $2\mu\text{m}$ to $10\mu\text{m}$ in purpose to investigate the effect of the green phosphor size to the optical performance of the MCW-LEDs. In the simulation stage in the Light Tools, we set the refractive index of the green and yellow phosphors at 1.42 and 1.83, respectively. The average radius of the phosphor particles is $7.25\mu\text{m}$, and the refractive index of the silicone glue was chosen 1.5. [12-15].

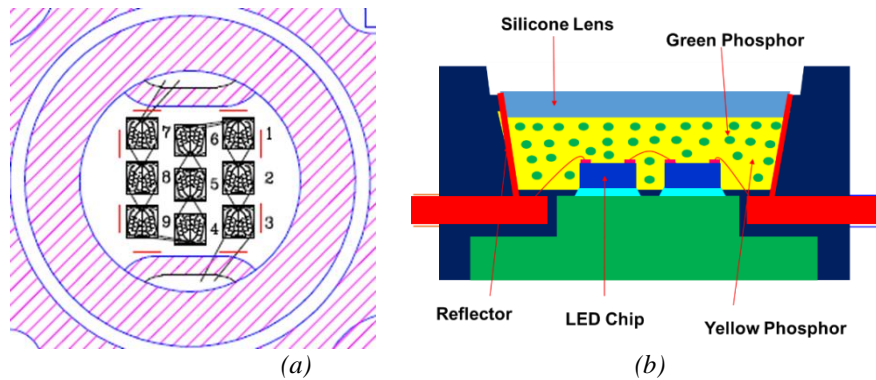


Fig. 1. The physical structure of the in-cup packaging WLEDs

2.2. Mathematical Description of Scattering Process

For more understanding the scattering process of the phosphor layer, the mathematical description is necessary to propose and demonstrate by applying Mie theory [16-22]. The scattering coefficient $\mu_{sca}(\lambda)$ (mm^{-1}), the absorption coefficient $\mu_{abs}(\lambda)$ (mm^{-1}), anisotropy factor $g(\lambda)$ (mm^{-1}), and reduced scattering coefficient $\delta_{sca}(\lambda)$ (mm^{-1}) can be computed by the below expressions (1), (2), (3), and (4):

$$\mu_{sca}(\lambda) = \int N(r)C_{sca}(\lambda, r)dr \quad (1)$$

$$\mu_{abs}(\lambda) = \int N(r)C_{abs}(\lambda, r)dr \quad (2)$$

$$g(\lambda) = 2\pi \int_{-1}^1 p(\theta, \lambda, r) f(r) \cos \theta d \cos \theta dr \quad (3)$$

$$\delta_{sca} = \mu_{sca} (1 - g) \quad (4)$$

In these equations, $N(r)$ indicates the distribution density of diffusional particles (mm^3). C_{abs} and C_{sca} is the absorption and scattering cross sections (mm^2), $p(\theta, \lambda, r)$ is the phase function, λ is the light wavelength (nm), r is the radius of diffusional particles (μm), and θ is the scattering angle ($^\circ$), and $f(r)$ is the size distribution function of the diffuser in the phosphorous layer. Moreover, $f(r)$ and $N(r)$ can be calculated by:

$$f(r) = f_{dif}(r) + f_{phos}(r) \quad (5)$$

$$N(r) = N_{dif}(r) + N_{phos}(r) = K_N \cdot [f_{dif}(r) + f_{phos}(r)] \quad (6)$$

$N(r)$ is composed of the diffusive particle number density $N_{dif}(r)$ and the phosphor particle number density $N_{phos}(r)$. In these equations, $f_{dif}(r)$ and $f_{phos}(r)$ are the size distribution function data of the diffuser and phosphor particle. Here K_N is the number of the unit diffuser for one diffuser concentration and can be calculated by the following equation:

$$c = K_N \int M(r) dr \quad (7)$$

Where $M(r)$ is the mass distribution of the unit diffuser and can be proposed by the below equation:

$$M(r) = \frac{4}{3} \pi r^3 [\rho_{dif} f_{dif}(r) + \rho_{phos} f_{phos}(r)] \quad (8)$$

Here $\rho_{dif}(r)$ and $\rho_{phos}(r)$ are the density of diffuser and phosphor crystal [26-30]. In Mie theory, C_{sca} and C_{abs} can be obtained by the following expressions:

$$C_{sca} = \frac{2\pi}{k^2} \sum_0^\infty (2n+1) (|a_n|^2 + |b_n|^2) \quad (9)$$

$$C_{ext} = \frac{2\pi}{k^2} \sum_1^\infty (2n+1) \text{Re}(a_n + b_n) \quad (10)$$

$$C_{abs} = C_{ext} - C_{sca} \quad (11)$$

Where $k = 2\pi/\lambda$, and a_n and b_n are the expansion coefficients with even symmetry and odd symmetry, respectively. They can be calculated by:

$$a_n(x, m) = \frac{\psi_n'(mx)\psi_n(x) - m\psi_n(mx)\psi_n'(x)}{\psi_n'(mx)\xi_n(x) - m\psi_n(mx)\xi_n'(x)} \quad (12)$$

$$b_n(x, m) = \frac{m\psi_n'(mx)\psi_n(x) - \psi_n(mx)\psi_n'(x)}{m\psi_n'(mx)\xi_n(x) - \psi_n(mx)\xi_n'(x)} \quad (13)$$

Where $x = k.r$, m is the refractive index, and $\psi_n(x)$ and $\xi_n(x)$ are the Riccati - Bessel function.

Moreover, the phase function $p(\theta, \lambda, r)$ can be calculated according to:

$$p(\theta, \lambda, r) = \frac{4\pi\beta(\theta, \lambda, r)}{k^2 C_{sca}(\lambda, r)} \quad (14)$$

Here $\beta(\theta, \lambda, r)$ is the dimensionless scattering function, which is obtained by the scattering amplitude functions $S_1(\theta)$ and $S_2(\theta)$.

$$\beta(\theta) = (1/2)[|S_1(\theta)|^2 + |S_2(\theta)|^2] \quad (15)$$

$$S_1(\theta) = \sum_{n=1}^{\infty} \frac{2n+1}{n(n+1)} \left[a_n \frac{P_n^1(\cos\theta)}{\sin\theta} + b_n \frac{dP_n^1(\cos\theta)}{d\theta} \right] \quad (16)$$

$$S_2(\theta) = \sum_{n=1}^{\infty} \frac{2n+1}{n(n+1)} \left[b_n \frac{P_n^1(\cos\theta)}{\sin\theta} + a_n \frac{dP_n^1(\cos\theta)}{d\theta} \right] \quad (17)$$

Where $P_n^1(\cos\theta)$ is the associated Legendre polynomial [16-22].

3. Results and discussions

In this section, the influence of the green phosphor size to the CRI and CQS of the MCW-LEDs is presented and investigated. In the first stage, the scattering, reduce scattering, and backscattering coefficients of the green phosphor in connection with its size is simulated by the Mat Lab software. Fig. 2 illustrate the scattering coefficient of the green phosphor versus the particle's size. It is found that the scattering at wavelengths of 453nm, 555nm crucial grew with increasing the particle. The research results show that the quality of the white light from MCW-LEDs can be enhanced by varying the size of the green phosphor particle. This can be based on the excellent absorption ability for the blue light from LED by the green phosphor particle. Moreover, Fig. 3 shows the same reduced scattering coefficient of the green phosphor at wavelengths 453nm, 555nm. It indicated that the scattering stability of the green-emitting $\text{CaF}_2:\text{Ce}^{3+}, \text{Tb}^{3+}$ phosphor showed the great uses for controlling the color quality of the in-cup packaging WLEDs. Fig. 5 showed the influence of the green-emitting $\text{CaF}_2:\text{Ce}^{3+}, \text{Tb}^{3+}$ phosphor's concentration on the angular scattering amplitudes of the in-cup packaging WLEDs at wavelengths 453nm, 555nm. From the figure, we can see huge massive influence of the green-emitting $\text{CaF}_2:\text{Ce}^{3+}, \text{Tb}^{3+}$ phosphor's concentration on the angular scattering amplitudes. The angular scattering amplitudes at wavelengths 453nm more extensive larger than at wavelengths 555nm. From the analysis the scattering process in the phosphor layer of the in-cup packaging WLEDs, the results indicated that the involvement of the green-emitting $\text{CaF}_2:\text{Ce}^{3+}, \text{Tb}^{3+}$ phosphor into the phosphor compounding could play a major role in controlling the optical properties of the in-cup packaging WLEDs [15].

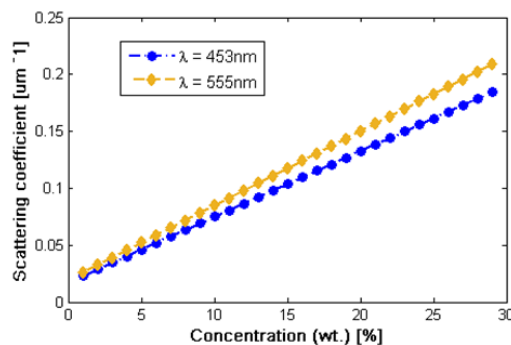


Fig. 2 The scattering coefficient of the green-emitting $\text{CaF}_2:\text{Ce}^{3+}, \text{Tb}^{3+}$ phosphor at wavelengths of 453nm, 555nm.

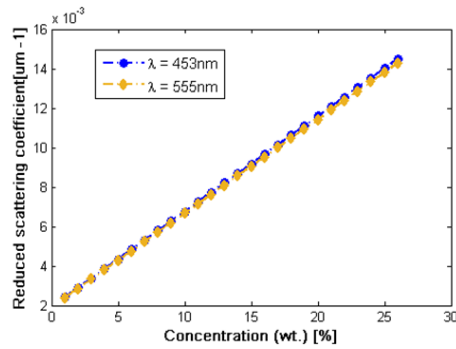


Fig. 3 The reduced scattering coefficient of the green-emitting $\text{CaF}_2:\text{Ce}^{3+}, \text{Tb}^{3+}$ phosphor at wavelengths of 453nm, 555nm.

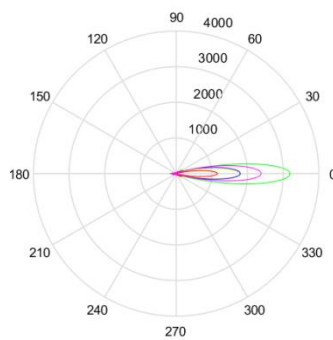


Fig. 4 The angular scattering amplitudes of the green-emitting $\text{CaF}_2:\text{Ce}^{3+}, \text{Tb}^{3+}$ Phosphor

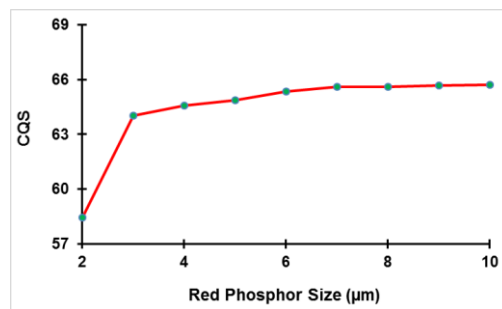


Fig. 5. The CRI of the 7000 K in-cup packaging MCW-LEDs by adding the green-emitting $\text{CaF}_2:\text{Ce}^{3+}, \text{Tb}^{3+}$ phosphor particles

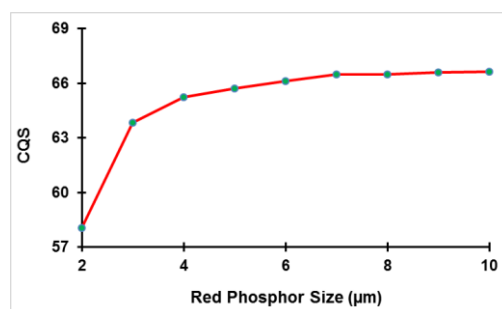


Fig. 6. The CRI of the 8500 K in-cup packaging MCW-LEDs by adding the green-emitting $\text{CaF}_2:\text{Ce}^{3+}, \text{Tb}^{3+}$ phosphor particles

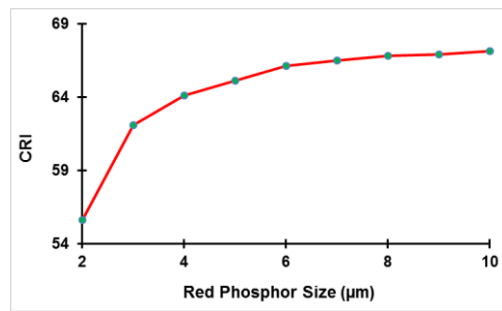


Fig. 7. The CRI of the 7000 K in-cup packaging MCW-LEDs by adding the green-emitting $\text{CaF}_2:\text{Ce}^{3+}, \text{Tb}^{3+}$ phosphor particles

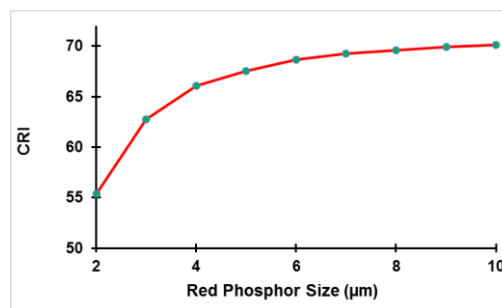


Fig. 8. The CRI of the 8500 K in-cup packaging MCW-LEDs by adding the green-emitting $\text{CaF}_2:\text{Ce}^{3+}, \text{Tb}^{3+}$ phosphor particles

Furthermore, we use the commercial Light Tools software to investigate the influence of the green-emitting $\text{CaF}_2:\text{Ce}^{3+}, \text{Tb}^{3+}$ phosphor's size on CQS and CRI of the 7000K, and 8500K in-cup packaging WLEDs. The size of the green phosphor is increased from $1\mu\text{m}$ to $10\mu\text{m}$ continuously. Fig. 4 and 5 illustrate the CQS of the 7000K, and 8500K in-cup packaging WLEDs on the increasing the green-emitting $\text{CaF}_2:\text{Ce}^{3+}, \text{Tb}^{3+}$ phosphor's size, respectively. Furthermore, Fig. 6 and 7 present the influence of particle size on CRI of the 7000K and 8500K in-cup packaging WLEDs. These results indicated that the CRI and CQS crucially increased while the size of the green-emitting $\text{CaF}_2:\text{Ce}^{3+}, \text{Tb}^{3+}$ phosphor rose continuously from $1\mu\text{m}$ to $10\mu\text{m}$. In this results, the scattered light of each particle in PC-LEDs is different, resulting in varying the optical properties of W-LEDs.. From the results, the involvement and the scattering process of the green-emitting $\text{CaF}_2:\text{Ce}^{3+}, \text{Tb}^{3+}$ phosphor could be playing an essential role in enhancing the optical properties of the in-cup packaging WLEDs.

4. Conclusions

In this paper, we investigate the effect of the green-emitting $\text{CaF}_2:\text{Ce}^{3+}, \text{Tb}^{3+}$ phosphor's size on CRI and CQS of the 7000K, 8500K in-cup packaging MCW-LEDs. From research results, the CQS and CRI were significantly increased while the size of the green-emitting phosphor varied from 2 to $10\mu\text{m}$. The CRI and CQS can obtain the optimal value at 67 and 65, respectively. The simulation results and the theoretical analysis agreed well with each other. This research can play the primary role in the development of the manufacturing MCW-LEDs in the future time.

Acknowledgments

The authors appreciate the support of Professor Hsiao-Yi Lee, Department of Electrical Engineering, National Kaohsiung University of Applied Sciences, Kaohsiung, Taiwan.

References

- [1] LED Packaging for Lighting Applications, Design of LED Packaging Applications p. 215–315. 2011. doi:10.1002/9780470827857.ch6.
- [2] Gibney, Elizabeth, *Nature* **514**(7521), 152 (2014).
- [3] Liu, Zong-Yuan, Sheng Liu, Kai Wang, Xiao-Bing Luo, *IEEE Transactions on Components and Packaging Technologies* **33**(4); 680 (2010)..
- [4] X. Luo, R. Hu, Chip packaging: Encapsulation of nitride LEDs. *Nitride Semiconductor Light-Emitting Diodes (LEDs)*, 441-481. (2014).
- [5] Luo, Xiaobing, Run Hu, Sheng Liu, Kai Wang, *Progress in Energy and Combustion Science* **56**, 1 (2016).
- [6] Y. Shuai, Y. He, N. T. Tran, F. G. Shi, *IEEE Photonics Technology Letters* **23**(3): 137 (2011), doi: 10.1109/LPT.2010.2092759.
- [7] Fu Xing, Huai Zheng, Sheng Liu, and Xiaobing Luo, *Frontiers of Optoelectronics* **5**(2) 153 (2012).
- [8] Yu, Renyong, Shangzhong Jin, Songyuan Cen, Pei Liang, *IEEE Photonics Technology Letters* **22**(23), 1765 (2010).
- [9] S. Markus, T. Rosenthal, O. Oecklera, W. Schnick, *Critical Reviews in Solid State and Materials Sciences* **39**(3), 215 (2014).
- [10] L. Liu, R. J. Xie, N. Hirosaki, T. Takeda, C. Zhang, J. Li, X. Sun, *Science and Technology of Advanced Materials* **12**(3), (2011).
- [11] H. Yu, W. W. Zi, S. Lan, H. F. Zou, S. C. Gan, X. C. Xu, G. Y. Hong, *Materials Research Innovations*, **16**(4): 298 (2012).
- [12] Minh, Tran Hoang Quang, Nguyen Huu Khanh Nhan, Nguyen Doan Quoc Anh, Hsiao-Yi Lee. *Journal of the Chinese Institute of Engineers* **40**(4), 313 (2017).
- [13] Minh, Tran Hoang Quang, and Le Anh Vu. *Lecture Notes in Electrical Engineering AETA 2017 - Recent Advances in Electrical Engineering and Related Sciences: Theory and Application*, 213 (2017).
- [14] Minh, Tran Hoang Quang. *International Journal of Automation and Smart Technology* **8**(1), 35 (2018).
- [15] Nguyen Huu Khanh Nhan, Tran Hoang Quang Minh, Tan N. Nguyen, Miroslav Voznak. *Digest Journal of Nanomaterials and Biostructures* **12**(3), (2017).
- [16] Zhao, Bei, Dingyi Shen, Qinyue Tan, Jianfeng Tang, Xianju Zhou, Shanshan Hu, Jun Yang. *Journal of Materials Science* **52**(10), 5857 (2017).
- [17] Guo, Hai, Yue Guo, Hyeon Mi Noh, Byung Kee Moon, Sung Heum Park, Jung Hyun Jeong, Kwang Ho Kim, *Journal of Nanoscience and Nanotechnology* **16**(1), 1146 (2016).
- [18] Zhao, Bei, Dingyi Shen, Qinyue Tan, Jianfeng Tang, Xianju Zhou, Shanshan Hu, Jun Yang. *Journal of Materials Science* **52**(10), 5857(2017).
- [19] Mishchenko, Michael I., Larry D. Travis, and Andrew A. Lacis. 2002. *Scattering, Absorption, and Emission of Light by Small Particles*. Cambridge: Cambridge University Press.
- [20] Zhong, Jiajian, Mingyuan Xie, Zhigui Ou, Rui Zhang, Min Huang, Fuli Zhao. *Mie Theory Simulation of the Effect on Light Extraction by 2-D Nanostructure Fabrication. Symposium on Photonics and Optoelectronics (SOPO)*. 2011.
- [21] Sommer, Christian, Frank Reil, Joachim R. Krenn, Paul Hartmann, Peter Pachler, Hans Hoschopf, Franz P. Wenzl. *Journal of Lightwave Technology* **29**(15), 2285 (2011).
- [22] Jonasz, Miroslaw, Georges R. Fournier. "General Features of Scattering of Light by Particles in Water." *Light Scattering by Particles in Water*, p. 87, 2007.